Identification of Chemotherapeutic Dihydromyricetin With Enhanced Anti-tumor Activity and Biosafety for Muscle Invasive Bladder Cancer

Zijian Wang
Wuhan University Zhongnan Hospital
Zicheng Guo
Wuhan University Zhongnan Hospital
Wenjie You
Wuhan University Zhongnan Hospital
Wang Wang
Wuhan University Zhongnan Hospital
Fenfang Zhou
Wuhan University Zhongnan Hospital
Renjie Zhang
Wuhan University Zhongnan Hospital
Zhiwen He
Wuhan University Zhongnan Hospital
Hongbo Chen
enshi tujiazu miaozu zizhizhou zhongxin yiyuan: Central Hospital of Enshi Tujia and Miao Autonomous Prefecture
Xinghuan Wang (wangxinghuan@whu.edu.cn)
Wuhan University Zhongnan Hospital https://orcid.org/0000-0003-3497-0024

Research

Keywords: Dihydromyricelin, Anti-tumor activity, Biosafety, Bladder cancer, Epithelial- mesenchymal transition

Posted Date: August 9th, 2021

DOI: https://doi.org/10.21203/rs.3.rs-763057/v1

Abstract

Background: Muscle invasive bladder cancer (MIBC) is one of the most common malignant diseases in elderly men, such as veterans. Postoperative chemotherapy plays a vital role in preventing recurrence and metastasis of MIBC. However, fewer of chemotherapeutic drugs with remarkable anti-tumor activity and biosafety are available for clinical treatment.

Methods: In this work, a novel plant-derived drug, named as dihydromyricetin (DHM), was selected for postoperative chemotherapy of MIBC. The anti-tumor activity was evaluated using a series of in vitro tests, such as MTT assay, flow cytometry and western blot. Furthermore, a xenograft model of BALB/C57 nude mice was established to verify the good anti-tumor activity and biosafety of DHM in vivo.

Results: DHM could effectively inhibit the proliferation, survival and migration of MIBC cell, and promote apoptosis ($P<0.05$). Cytotoxic macrophage polarization from M0 to M1 was promoted by DHM treatment, and the hub genes in cell cycle and apoptosis signaling pathways were differential expressed. We also found that DHM could reverse the epithelial-mesenchymal transition (EMT) of MIBC cell. The in vivo results revealed that intravenous injection of DHM with a dose of 20 mg/kg for 7 times could significantly suppress the in vivo tumorigenesis of MIBC ($P<0.05$), while triggered no obvious drug side effects.

Conclusion: This work identified a novel chemotherapeutic DHM with remarkable anti-tumor activity and biosafety, which could serve as a promising alternative for postoperative chemotherapy of MIBC.

Background

The morbidity and mortality of bladder cancer (BCa) rank first in genitourinary malignancies with estimated 4.3×10^5 new cases and 1.7×10^5 deaths each year [1, 2]. According to the histopathological characteristics, BCa can be classified into 2 distinctive groups: muscle invasive BCa (MIBC) with high grade and non-muscle invasive BCa (NMIBC) with low grade [3, 4]. Clinicians and basic researchers have employed some laparoscope and da Vinci robot assisted operations to treat MIBC [5, 6]. However, therapeutic effects of MIBC are not fully satisfactory in clinic, and the survival time of MIBC patients is greatly affected by cancer recurrence and metastasis [7]. According to an epidemiological investigation, 5-year mortality rate of the MIBC patients without lymph node metastasis is approximately 18.6%, while that of the MIBC patients with lymph node metastasis is as high as 77.6% [2]. Thus, it is quite necessary to adopt postoperative interventions to inhibit the recurrence and metastasis of MIBC.

Routine intravenous chemotherapy is one of the most commonly used postoperative treatments among a widely range of tumors [8]. Powles et al. have reported a multi-center, phase 3 clinical study on altezizumab and platinum chemotherapy for locally advanced and metastatic urological carcinoma [9]. The available MIBC chemotherapeutic drugs in China are mainly composed of gemcitabine, vincristine, methotrexate and pirarubicin [10, 11]. Few drugs and their combinations can completely kill cancer cells in vivo, partly owning to the individual differences between MIBC patients. Currently, the study on anti-tumor drug is of increasing interest. Food and Drug Administration (FDA, USA) has approved at least 59

anti-tumor drugs whose response rate were assessed in more than 100 patients. Thus, we plan to screen a novel candidate drug with enhanced anti-tumor activity and biosafety for MIBC chemotherapy.

Lots of plant-derived drugs (PDD) have been proved to be biocompatible and non-toxic for in vivo applications [12]. It is estimated that thirteen antitumor PDD, such as camptothecin, paclitaxel, vincristine and colchicine, have obtained the U.S. new drug certificate since 1955 [13, 14]. Our research group focused on exploring novel MIBC chemotherapeutic drugs, like capsaicin, resveratrol, plumbagin and nicotinamide. We have reported that capsaicin could inhibit in vivo MIBC xenograft growth via FOXO3a mediated signaling pathways [15]. A large number of Chinese herbals with anti-tumor potential are recorded in traditional medical texts, including *Compendium of Materia Medica* [12]. In the past decades, some anti-tumor components have been extracted from crude drugs by chemical methods, and started next-generation of drug screening [16].

Dihydromyricetin (DHM), also named as ampelopsis, is a kind of natural plant-derived flavonoids. DHM can be extracted from the smashed ratten tea by distillation and vacuum crystallization, and then recrystallized in acetone solution. Similar with the other flavonoids, DHM possesses multiple pharmacological functions of anti-tumor, cardio-protection, anti-diabetes, and neuroprotection, et al [17]. Particularly, the anti-tumor function and mechanism of DHM has been investigated among lung cancer, ovarian cancer, colorectal cancer and triple negative breast cancer [18–20]. Xu et al. reported that DHM could significantly induce ovarian cancer cells apoptosis and effectively reverse p53 gene mediated chemotherapy resistance [21]. Tieng et al. reported that DHM could inhibit the invasion of the triple negative breast cancer by blocking extracellular matrix (ECM) degradation [22]. In addition, we previously found the proliferation inhibition effects of DHM against BCa cells. However, DHM has rarely been investigated for MIBC treatment, and the anti-tumor functions and mechanism remains to be uncovered.

In this work, DHM is selected as the candidate chemotherapeutic drug for MIBC chemotherapy. The anti-tumor activity and biosafety of DHM against MIBC cells are characterized by a series of in vitro and in vivo experiments, such as MTT assay, cell migration assay, flow cytometry, western blot, and histopathological analysis. It is assumed that DHM can inhibit the tumorigenesis of MIBC without causing obvious drug toxicity. This work will screen out a prospective chemotherapeutic drug, which can be used alone in practice, or further processed into nanomaterials for MIBC precise treatment.

Material And Methods

Reagents and chemicals

Commercial dihydromyricelin (DHM, $C_{15}H_{12}O_8$, analytical purity, CAS: 27200-12-0) was purchased from Macklin Biochemical Co., Ltd. (Shanghai, China). DHM was dissolved into dimethyl sulfoxide (DMSO) to obtain a stock solution with a concentration of 200 mM, and stored at -20℃ for further applications. DMSO, absolute ethanol, methanol, crystal violet, paraformaldehyde (PFA) and paraffin were obtained from Sinopharm Chemical Reagent Co., Ltd. (Shanghai, China). RPMI-1640 and DMEM high glucose

medium, fetal bovine serum (FBS), penicillin, streptomycin, and trypsin were purchased from Thermofisher Scientific Co., Ltd. (Waltham, MA, USA). The other chemical and biological reagents were used as received.

Bladder cancer cell lines

The muscle invasive bladder cancer (MIBC) cell lines (T24 and UMUC3) were purchased from the American Type Culture Collection (ATCC) (Manassas, VA, USA). T24 cell was maintained in RPMI-1640 complete medium supplied with 10% FBS and 100 U/mL penicillin/streptomycin solution. UMUC3 cell was maintained in DMEM high glucose complete medium containing FBS and antibiotics. T24 and UMUC3 cells were both cultured using a 37℃ humid incubator with 5% CO_2.

Cell viability and proliferation assay

In this study, MTT assay was performed to determine the appropriate DHM drug concentration for further in vitro evaluations. Briefly, T24 or UMUC3 cells were digested using 0.25% trypsin solution, and then centrifuged at 1200 rpm for 5 min. DHM stock solution with a concentration of 200 mM was diluted using complete medium until the desired DHM concentration (0, 5, 10, 20, 30 μM) was achieved. DHM working solutions were used to re-suspend cell precipitation, and adjust cell concentration to 1.5×10^4 cells/mL. 200 μL cell suspension was added into each well of 96 well plates. After incubated at 37℃ for 48 h, 20 μL MTT reagent was added, followed by incubation for another 4 h. After that, all liquids in the 96 plates were thoroughly wiped out, and 150 μL DMSO was added into each well. The value of optical density (OD) at a wavelength of 490 nm was detected using a microplate reader (SpectraMax@M2, MD, USA). The relative cell viability and 50% inhibiting concentration (IC50) were calculated [23]. To further assess the proliferation ability of MIBC cells, T24 and UMUC3 cells were co-incubated with DHM working solution (0, 5, 20 μM) for successive 5 days. At regular time intervals, the treated cells were taken out of the incubator, and the value of OD490 was detected. Six independent samples were calculated for statistical comparison.

Clonogenic survival assay

T24 and UMUC3 cells were collected and re-suspended into DHM working solutions (0, 5 and 20 μM). These cells were seeded onto 6 well tissue culture plates with cell density of 800 cells/well, and then cultured for 12 days. 4% paraformaldehyde (PFA) solution was added to fix the cells. After that, 1 mL 0.1% crystal violet solution was applied to visualize the cell clone. The images of cell clones were captured using a digital camera (A7R□, Sony, Japan), and the number of cell clones was counted from at least three independent sample.

Transwell chamber assay

In this work, transwell chambers (Millipore, Corning, USA) were used to investigate the migration ability of MIBC cells[24]. Briefly, DHM stock solution (200 mM) was diluted using FBS-free basic medium to 0, 5, 20 μM, respectively. The obtained solutions were suspended with T24 or UMUC3 cells with a concentration 4×10^5 cells/mL. 0.1 mL cell suspension was added into the upper layer of transwell chamber, and 0.7 mL

complete medium was added into the lower layer. After incubated at 37°C for 24 h, the un-migrated cells on the upper chamber layer were removed carefully using a cotton swab. The migrated cells were fixed with 4% PFA solution for 30 min, and then stained with 0.1% crystal violet solution for 15 min. The cell images were captured by an inverted fluorescence microscope (IX73, OLYMPUS, Japan), the IPP-6.0 software was used for quantitative analysis.

Wound healing assay

T24 and UMUC3 cells were seeded onto 6 well tissue culture plates with high cell density, and then cultured overnight until the cell confluence reached to 80%. A linear cell wound was created using 200 μL pipette tips. After washed twice by PBS solution, the culture plates were filled with DHM working solutions with a concentration of 0, 5, 20 μM, respectively. At regular time intervals, three representative images of wound site were captured and analyzed using an inverted fluorescence microscope (IX73, OLYMPUS, Japan).

Flow cytometric analysis

Cell cycle

The cell cycle analysis was carried out in accordance with our precious report [25]. T24 and UMUC3 cells were co-incubated with DHM working solutions (0, 5, 20 μM) for 48 h, and then collected into 1.5 mL centrifuge tubes. The obtained cells were washed using PBS solution for three times. Cell cycle staining kit was purchased from Multi Sciences Co., Ltd. (Hangzhou, China). 1 mL DNA staining solution and 10 μL permeabilization solution was added into each tube. After incubated in the dark place for 30 min, the cell cycle was detected using a flow cytometry (CytoFLEX, Beckman, USA). At least three independent samples were tested in each group.

Cell apoptosis

MIBC cells were treated with DHM working solutions (0, 5, 20 μM) for 48 h, and then collected into 1.5 mL tubes for apoptosis staining. The Annexin V-FITC/PI apoptosis kit was obtained from BD Biosciecnes Co., Ltd. (San Jose, USA). The DHM treated cells were re-suspended in the 1 × binding buffer, and then stained with Annexin V-FITC for 15 min and PI for another 10 min. The apoptosis rate of all samples was detected using a flow cytometry (CytoFLEX, Beckman, USA). At least three independent samples were tested in each group.

Phenotypic characterization

T24 cells were incubated with DHM working solutions (0, 5, 20 μM) for 12 h, and the supernatant was collected for phenotypic characterization. Human monocytic leukemia cell line (THP-1) was seeded in 6 well tissue culture plates with a density of 1×10^6 cells/well. After incubated with the supernatant for 24 h, the THP-1 cells were collected and treated with CD11b/c-APC, CD86-FITC, CD80-PE. The stained cells were then analyzed using a flow cytometry. The percentage of positive cells indicated the expression degree of the surface markers, and calculated from three independent samples [26].

Quantitative real-time PCR

According to previous report [27], the total RNA molecules from the treated MIBC cells were isolated using a HiPure RNA Mini Kit (Magen, China). The RNA concentration was then measured using an ultraviolet spectrophotometer (Nanodrop 2000, Thermo, USA). The reverse transcription reaction was carried out, and the obtained cDNA was used for quantitative real-time PCR (qRT-PCR). The iQTM SYBR®Green Supermix was purchased from Bio-Rad Co., Ltd. (Shanghai, China) and applied for qRT-PCR. Primer sequences used in this work are listed in Table S1.

Western blot and immunofluorescence (IF) staining

T24 and UMUC3 cells were incubated with DHM working solutions (0, 5, 20 μM) for 48 h before they were harvested for western blot analysis. The treated cells were completely lysed in 1 mL RIPA buffer containing 20 μL phosphatase and protease inhibitor mixture. The lysis supernatant was collected after centrifuged at 1.2×10^4 g for at least 15 min. The total protein concentration was evaluated using a BCA protein assay kit (Abcam, China). The protein samples were denatured and separated by 7.5–15% SDS - PAGE gels, and then transferred to a PVDF membrane (Millipore, USA). The PVDF membranes were blocked using 5% fat-free milk for 2 h and incubated with primary antibodies overnight and secondary antibodies for 2 h. The primary and secondary antibodies used in this work are listed in Table S2. The enhanced chemiluminescence kit was purchased from BD Biosciecnes Co., Ltd. (San Jose, USA). The protein bands were detected using a ChemiDoc™ MP Imaging System (Bio-Rad, USA). IF staining of Ki67 protein were performed according to the general protocols, and accomplished by Biofavor Biotech Co., Ltd. (Wuhan, China). The cell images of IF staining were captured by an inverted fluorescence microscope (IX73, OLYMPUS, Japan).

In vivo xenograft experiments

This work was carried out in accordance with the declaration of Helsinki. Six BALB/C57 nude mice, aging about 3 weeks, were purchased from WQJX Bio-Technology Co., Ltd. (Wuhan, China). These animals were quarantined in SPF experimental facility for 7 days to adapt the new environment.

200 μL T24 cells (1.5×10^7 cells/mL in PBS) were subcutaneously injected into the mice. The animals were fed for 15 days before DHM drug injection. DHM was firstly dissolved in absolute alcohol with a concentration of 10 mg/mL, and then diluted using normal saline to prepare the DHM working solution. DHM working solution was injected at a dose of 20 mg/Kg every third day for 21 days. For blank control, animals were injected with normal saline containing equivalent alcohol. Tumor size of the treated animals was measured using a vernier caliper, and then used to calculate the tumor volume (mm^3) as $A_L \times A_W^2 \times 0.5$, where A_L and A_W refers to the length and width of the tumors, respectively. After sacrificing the animals, all tumor samples, blood samples and organs samples including heart, liver, spleen, lung, kidney and brain, were harvested for further tests [28].

The tumor samples and organs were fixed with 4% paraformaldehyde (PFA) solution for 48 h. These samples were embedded by paraffin and then sliced into 4 μm sections. Hematoxylin-eosin (HE) and Masson's trichrome (MT) staining, immunofluorescence (IF) staining of Ki67, and TUNEL assay were performed according to the general protocols. An inverted fluorescence microscope (IX73, OLYMPUS, Japan) was used for data acquisition.

The concentration of alanine aminotransferase (ALT), aspartate aminotransferase (AST), γ-glutamyl transpeptidase (GGT), creatinine (CRE), and total bilirubin (TBIL) was detected. Commercial kits were purchased from BOSTER Biotechnology Co., Ltd. (Wuhan, China). The blood samples were centrifuged at 3000 rpm for 5 min, and then diluted using distilled water. The test was performed according to the manufacturers' protocols. At least three samples were used for statistical analysis

Statistical analysis

The data from no less than three independent biological evaluations were expressed as mean ± standard deviation. One-way ANOVA as well as post hoc Tukey's test was applied for statistical analysis. $p < 0.05$ was considered to be statistically different.

Results

DHM concentration for in vitro evaluations

To screen out the appropriate DHM drug concentration for in vitro experiments, T24 and UMUC3 cells were co-incubated with DHM solution (0, 5, 10, 20 and 30 μM), and the relative viability of treated cells was assessed by MTT assay. As shown in Fig. 1a-b, the relative cell viability after DHM treatment decreased significantly along with an increase of DHM concentration from 0 to 30 μM, suggesting that DHM possessed the potential anti-tumor activity against MIBC. The IC50 values of DHM were 22.3 μM for T24 cell, and 16.7 μM for UMUC3 cell. Thus, we intended to set three independent groups in the following experiments: high dose group (20 μM), low dose group (5 μM) and blank control group (0 μM).

DHM inhibited MIBC cell proliferation in a dose-dependent manner

MTT assay was also applied to evaluate the anti-proliferation activity of DHM against MIBC cells. The proliferation curves of T24 and UMUC3 cells are shown in Fig. 1c-d. The optical density (OD) value declined significantly as the DHM concentration increased. At the 5th day, the OD values of T24 cell were 1.31 ± 0.10 for 0 μM group, 1.03 ± 0.10 for 5 μM group and 0.49 ± 0.04 for 20 μM group. Meanwhile, the OD values of UMUC3 cell were 1.34 ± 0.16 for 0 μM group, 1.03 ± 0.12 for 5 μM group and 0.36 ± 0.04 for 20 μM group. Significant difference was observed between each group ($P < 0.05$). In conclusion, DHM possessed a dose-dependent anti-proliferation activity against MIBC cells.

DHM induced cell cycle arrest

To investigate the mechanism of anti-proliferation activity of DHM, cell cycle analysis, qRT-PCR and western blot assay were performed. The results of cell cycle analysis are shown in Fig. 2a-d, the percentage of MIBC cells in G0/G1 phase was significantly increased after DHM treatment ($P < 0.05$). For T24 cell, the percentage of G0/G1 phase cells increased from 51.3 ± 0.4% (0 μM group) to 62.8 ± 0.1% (5 μM group) and 62.7 ± 0.1% (20 μM group). For UMUC3 cell, the percentage of G0/G1 phase cells increased from 53.7 ± 0.7% (0 μM group) to 56.5 ± 1.3% (5 μM group) and 60.1 ± 0.3% (20 μM group). This phenomenon suggested that DHM could effectively induce cell cycle arrest, which played a vital role in tumor development. The expression level of cell cycle related genes (P53, CDK2, CDK4, Cyclin D1 and Cyclin E1) was tested by qRT-PCR assay. As shown in Fig. 2e-f, P53 gene in the 5 μM and 20 μM groups was up-regulated while the other genes were significantly down-regulated ($P < 0.05$). The results of western blot also exhibited an obvious down-regulation of CDK2, CDK4, Cyclin D1 and Ki67 proteins in both T24 and UMUC3 cells (Fig. 2g-h). CDK2/4 and Cyclin D1/E1 can form the hub complexes to participate in multiple biological signaling pathways, and drive cell cycle from G0/G1 phase to S phase. Thus, the abnormal expression of these genes might interrupt the cell cycle pathway, and eventually lead to the proliferation inhibition effect among MIBC cells. Ki67 is one of the markers for cell proliferation activation state. As shown in Fig. 2i-j, fluorescence intensity (FSI) of the T24 and UMUC3 cells was both faded away after DHM treatment. This phenomenon has further confirmed that DHM could inhibit MIBC cells proliferation.

DHM activated the apoptosis pathway

The cell apoptosis was evaluated using a Annexin V-FITC/PI staining method. The representative images of flow cytometry are shown in Fig. 3a-b, and its quantitative results are shown in Fig. 3c-d. After co-incubated with DHM for 48 h, the apoptosis rate of T24 and UMUC3 cells were both significantly improved ($P < 0.05$). For T24 cell, the cell apoptosis rate increased from 8.7 ± 0.7% (0 μM group) to 12.3 ± 1.1% (5 μM group) and 19.9 ± 5.5% (20 μM group). For UMUC3 cell, the cell apoptosis increased from 5.2 ± 0.5% (0 μM group) to 6.3 ± 0.1% (5 μM group) and 7.6 ± 0.9% (20 μM group). Apoptosis is an independent and programmed way of death, which is regulated by many genes like caspase 3/6/9. Particularly, caspase 3 is the most important protein-cutting enzyme in apoptosis pathway. As shown in Fig. 3e-f, the relative mRNA expression of caspase 3, caspase 6 and caspase 9 in T24 and UMUC3 cells were significantly up-regulated by DHM treatment ($P < 0.05$). Furthermore, the results of western blot analysis also exhibited an obvious growth trend in caspase 3/6/9 proteins (Fig. 3g-h). In conclusion, DHM could promote MIBC cells apoptosis via activating the transcription and translation of caspase 3/6/9.

DHM Induced the polarization of M1 macrophages

The synergistic effects of tumor killing and immune response was evaluated by flow cytometry. CD80 and CD86 are the markers of M1 macrophages, and CD11b/c is the marker of monocytes. The polarization from initial monocytes to M1 macrophages could be used to indicate immune activation during chemotherapy. The results of CD80 staining are shown in Fig. S1a-b. The percentage of CD80 positively stained cells increased greatly after DHM treatment ($P < 0.05$). The percentage of CD80

positively stained cells was 0.51 ± 0.48% in the 0 μM group, and then decreased to 1.52 ± 0.4% and 32.1 ± 4.1% in the 5 μM group and 20 μM group, respectively. The results of CD86 staining are shown in Fig. S1c-d, and exhibited the similar growth trend. The polarization from monocytes to M1 macrophages could be motivated by foreign antigens such as cell debris. In this study, DHM killed MIBC cells, resulting in increased cell debris, and eventually led to M1 macrophage polarization.

DHM blocked the survival and migration of MIBC cells

In this work, clonogenic survival assay was adopted to investigate the survival ability of MIBC cells as reported before [29]. The images of T24 and UMUC3 cell clones are shown in Fig. 4a, and the quantitative results of clone number are shown in Fig. 3b-d. The clone number of T24 cells was 78.3 ± 9.5 in the 0 μM group, and then decreased to 39.0 ± 9.2 and 18.3 ± 3.5 in the 5 μM group and 20 μM group, respectively. For UMUC3 cell, the clone number was 147.7 ± 12.5 in the 0 μM group, and then decreased to 73.4 ± 7.1 and 14.4 ± 6.5 in the 5 μM group and 20 μM group, respectively. It could be concluded that DHM inhibited BCa cell survival significantly ($P < 0.05$)

Transwell chamber assay and wound healing assay were both performed to evaluate the migration ability of MIBC cells. The representative images in transwell chamber assay are shown in Fig. 4d. The migrated cells at the lower layer of transwell chamber were photographed and counted. The relative number of migrated T24 or UMUC3 cells was both declined after DHM treatment (Fig. 4e-f). The representative images of T24 and UMUC3 cells in wound healing assay are shown in Fig. 4g-i, and the corresponding statistical results of wound healing rate are shown in Fig. 4h-j The result of wound healing assay was in consistent with that of transwell chamber assay. In conclusion, the survival and migration abilities of MIBC cells could be effectively blocked by DHM treatment.

DHM reversed epithelial-mesenchymal transition (EMT) in MIBC cells

DHM can effectively inhibit in vitro migration of MIBC cells, but its' mechanism remains to be unknown. EMT is an important biological process for tumor cells to gain the phenotypic characteristics and metastatic potential of mesenchymal cells. Thus, we intended to investigate the expression of EMT markers, so as to uncover the mechanism of migration inhibition. Mesenchymal markers (N-cad, Vimentin and Snail) and epithelial marker (E-cad) were chosen for expression analysis. As shown in Fig. 5a-b, the relative expression of E-cad gene in both T24 and UMUC3 cells were significantly up-regulated ($P < 0.05$), while that of N-cad, Vimentin and Snail genes were all significantly down-regulated by DHM treatment ($P < 0.05$). The results of western blot also exhibited similar tendency in both T24 and UMUC3 cells (Fig. 5c-d). Generally, the EMT process in MIBC cells was successfully reversed by DHM treatment, which might lead to migration inhibition eventually.

DHM suppressed in vivo tumor growth with biosafety

A xenograft mouse model was created by subcutaneously transplanting T24 cells into the treated animals. The DHM working solution and the blank control solution were prepared and injected

intravenously to imitate clinical chemotherapy. The dose of DHM for in vivo application was set to be 20 mg/kg, and the frequency of injection was set to be every third day. After 21 days of chemotherapy, the tumor samples were collected for histological analysis. Blood samples and m ain organs (heart, liver, spleen, lung, kidney, and brain) of the animals were also harvested for in vivo biosafety evaluations.

The object image of tumor bearing mice is shown in Fig. 6a, and the photo of tumor samples dissected in the 36th day is shown in Fig. 6b. It was observed that the tumor volume in the DHM group grew much lower than that in the blank control group (Fig. 6c). Compared with blank control, the average tumor weight has decreased from 0.56 ± 0.07 g to 0.17 ± 0.06 g (Fig. 6d), significant difference was observed ($P < 0.001$). The HE staining of tumor samples from three pairs of treated animals also confirmed a definitive anti-tumor activity of DHM against MIBC (Fig. 6e).

In vivo proliferation and apoptosis of the treated MIBC xenografts were further evaluated by immunofluorescence staining and TUNEL assay. As shown in Fig. S2a, Ki67 protein was dyed red and located in the nucleus, and less Ki67 positively stained cells were found in DHM group. Ki67 is a member of cell cycle related proteins, and its' up-regulation usually leads to rapid proliferation. This result suggested that the proliferation ability of the MIBC xenografts was inhibited by DHM treatment. The images of TUNEL assay are shown in Fig. S2b. More positively stained cells appeared in DHM group, further indicating that the apoptosis of MIBC xenografts was motivated by DHM treatment.

In vivo biosafety of the DHM chemotherapy was evaluated using a histological method [27]. The HE and Masson staining of the organ samples were performed, and the corresponding images are shown in Fig. 6f-g. Compared with blank control, the histological structures in DHM group were slightly changed. Typically, pulmonary edema and pulmonary interstitial dilatation were observed. Besides, cardiac myocytes are enlarged and disorganized, which could be attributed to pulmonary cardiac compensatory hyperplasia. Mild inflammatory infiltration was found in heart, lung and kidney. These results suggested that DHM had potential organ toxicity, mainly targeting lung tissue. It is worth mentioning that the toxicity of DHM may be caused by overdose, and the ideal dose of DHM needs to be optimized in subsequent experiments. In vivo hemocompatibility of the DHM chemotherapy was also carried out as reported before [30]. The blood biochemical indicators, such as ALT, AST, GGT, CRE and TBIL, were detected using an enzyme linked immunosorbent assay. The corresponding results are shown in Fig. S3a-b. Compared with blank control, there was no significant difference in each indicator of the DHM group ($P > 0.05$), suggesting that DHM chemotherapy was non-toxic towards blood samples. Our results from in vivo tests preliminarily demonstrated that DHM chemotherapy could significantly suppress MIBC tumorigenesis while trigger no obvious drug toxicity. This study has screened out a plant-derived drug, which was desirable for the application of MIBC chemotherapy.

Discussion

Original advances in the biomedical fields, especially innovative drug, technology and equipment, have greatly improved the existing clinical diagnosis and treatment systems [31, 32]. For example, the

application of chemotherapeutic agents has prolonged the survival of tumor patients significantly. Currently, the available chemotherapeutic agents are mainly composed of platinum compound, hormone, antibody, alkylating agent, anti-metabolic drug, plant-derived drug, et al [33]. Particularly, some agents like paclitaxel, cisplatin and gemcitabine, have been widely used in clinic [33, 34]. MIBC is a malignant tumor prone to recurrence and metastasis, and the effect of post-operative chemotherapy of MIBC is far from satisfactory. Some methods like combination chemotherapy, neoadjuvant chemotherapy and bladder irrigation, have been developed to solve this problem [35]. It is prospective to explore more candidate agents with excellent anti-tumor activity and biosafety for MIBC chemotherapy.

Dihydromyricetin (DHM) is a natural flavonoid which was exacted from a Chinese herbal medicine named as ratten tea [17]. Similar with the other PPDs, DHM possesses remarkable advantages in biocompatibility and non-toxicity. DHM exhibits excellent anti-tumor activity against lung cancer, ovarian cancer, colorectal cancer, cutaneous squamous cell carcinoma, etc [21, 46]. However, the in vitro and in vivo applications of DHM for MIBC chemotherapy have rarely been reported. In this study, we firstly found that DHM could inhibit the proliferation and migration of MIBC (T24 and UMUC3) cells, and promote cell apoptosis. Interestingly, these anti-tumor properties of DHM were modulated in a dose-dependent manner. The results of in vivo tests further revealed that DHM could effectively suppress the growth of xenograft without causing obvious toxicity. Thus, it could be presumed that DHM serve as a promising candidate for MIBC chemotherapy. However, the molecular mechanism and biosafety of DHM needed to be further characterized before clinic application.

The anti-tumor mechanism of DHM varies greatly from cancer to cancer. For example, Zhiqiang Zhao et al. have demonstrated that DHM could suppress the tumorigenesis of osteosarcoma via modulating P38 (MAPK) and AMPKα/GSK3β/Sox2 signaling pathway [17]. Another literature from Bin Liu et al. have reported that DHM could induce hepatocellular carcinoma cell apoptosis, and further slowed production of reactive oxygen species (ROS) [36]. In general, the anti-tumor mechanism of DHM may be involved into the following biological processes, such as cell cycle arrest, apoptosis, ferroptosis, autophagy, ROS production, EMT and angiogenesis inhibition, et al [37]. Our group had screened the differentially expressed genes between carcinoma tissue and para-carcinoma tissue of MIBC [25, 29], and then verified the function/mechanism of the candidate genes. We found that cell cycle regulation, apoptosis and EMT were highly correlated with MIBC development and progression. In this work, we have detected the expression of hub genes or markers in the processes of cell cycle arrest, apoptosis and EMT. It was observed that the cell cycle and apoptosis signaling pathways were both interrupted by DHM treatment, and the EMT in BCa cells was successfully reversed. Other unknown mechanisms of DHM will be investigated in the future work.

Biosafety evaluation is one of the core components in the preclinical study of pharmaceutical preparations, nanomaterials and implantable devices [38, 39]. Zhang et al. have put forward a commonly used histological method to evaluate drug toxicity. Briefly, the treated animals were executed, and the organs like heart, liver, spleen, lung, kidney and brain were dissected for histological analysis. In this work, the tumor bearing assay and in vivo biosafety evaluations were performed at the same time. Intravenous

injection of DHM with a dose of 20 mg/kg for 7 times successfully suppressed the xenograft growth, but led to potential organ toxicity to lung tissues. In order to minimize the side effects, the dose and frequency of DHM injection in the animal experiments should be cut down. On the other hand, DHM could be modified and functionalized by biomaterials science and technology. For example, DHM could be capsuled into tumor cell derived exosomes, and then targeted to cancer cells and kill them precisely [40, 41]. A large number of tumor nano-platforms, such as exosome, cell membrane vesicle, metal-organic framework (MOF), carbon nanotube (CNT) and microfluidic, has made it possible for precision medicine [42–45].

Conclusions

Post-operation chemotherapy has been widely applied for MIBC patients. Nevertheless, few chemotherapy drugs can achieve good curative effects. In this work, DHM was screened out to be a novel anti-tumor drug against MIBC, and the application potential was characterized in vitro and in vivo. We found that DHM could not only inhibit the proliferation and migration of MIBC cells, but also promote apoptosis, and suppress the growth of xenograft without obvious toxicity. Our current work provided a prospective chemotherapy drug, which could be used alone or further processed into biomaterials for MIBC precise treatment.

Abbreviations

PDD: plant-derived drugs; DHM: dihydromyricetin; MIBC: muscle invasive bladder cancer; NMIBC: non muscle invasive bladder cancer; EMT: epithelial-mesenchymal transition; BCa: bladder cancer; FDA: Food and Drug Administration; ECM: extracellular matrix; DMSO: dimethyl sulfoxide; PFA: paraformaldehyde; FBS: fetal bovine serum; ATCC: American Type Culture Collection; IF: immunofluorescence; HE: Hematoxylin-eosin; MT: Masson’s trichrome; ALT: alanine aminotransferase; AST: aspartate aminotransferase; GGT: γ-glutamyl transpeptidase; CRE: creatinine; TBIL: total bilirubin; MOF: metal-organic framework; CNT: carbon nanotube.

Declarations

Supplementary information

The online version contains supplementary material are available.

Acknowledgements

Not applicable.

Competing Interests

The authors declare that there are no conflicts of interest.

Acknowledgments

Not applicable.

Authors' contributions

WZ, GZ and YW carried out literature searches, performed experiments, prepared figures, did data interpretation and writing; WW, ZF, ZR and HZ performed experiments and editing; CH and WX conceptualized the paper, prepared figures, did writing and editing. All the authors read and approved the final manuscript.

Funding

This work was financially supported by the Improvement Project for Theranostic Ability on Difficulty Miscellaneous Disease (Tumor) from National Health Commission of China (ZLYNXM202006), the Chinese Central Special Fund for Local Science and Technology Development of Hubei Province (2018ZYYD023), and the Science and Technology Department of Hubei Province Key Project (2018ACA159).

Availability of data and materials

The data and materials are available from the corresponding author upon reasonable request.

Ethics approval and consent to participate

This study was approved by the Animal Care & Welfare Committee of Wuhan University School of Basic Medical Sciences (No: 201816).

Consent for publication

Not applicable.

Competing interests

The authors have no competing interests to declare.

References

1. Torre LA, Bray F, Siegel RL, Ferlay J, Lortet-Tieulent J, Jemal A. Global cancer statistics, 2012. CA Cancer J Clin. 2015; 65: 87-108. https://doi.org/10.3322/caac.21262
2. He W, Zhong G, Jiang N, Wang B, Fan X, Chen C, et al. Long noncoding RNA BLACAT2 promotes bladder cancer-associated lymphangiogenesis and lymphatic metastasis. J Clin Invest. 2018; 128: 861-75. https://doi.org/10.1172/JCI96218

3. Galsky MD, Wang H, Hahn NM, Twardowski P, Pal SK, Albany C, et al. Phase 2 Trial of Gemcitabine, Cisplatin, plus Ipilimumab in Patients with Metastatic Urothelial Cancer and Impact of DNA Damage Response Gene Mutations on Outcomes. Eur Urol. 2018; 73: 751-9. https://doi.org/10.1016/j.eururo.2017.12.001
4. Szabados B, van Dijk N, Tang YZ, van der Heijden MS, Wimalasingham A, Gomez de Liano A, et al. Response Rate to Chemotherapy After Immune Checkpoint Inhibition in Metastatic Urothelial Cancer. Eur Urol. 2018; 73: 149-52. https://doi.org/10.1016/j.eururo.2017.08.022
5. Parekh DJ, Reis IM, Castle EP, Gonzalgo ML, Woods ME, Svatek RS, et al. Robot-assisted radical cystectomy versus open radical cystectomy in patients with bladder cancer (RAZOR): an open-label, randomised, phase 3, non-inferiority trial. The Lancet. 2018; 391: 2525-36. https://doi.org/10.1016/s0140-6736(18)30996-6
6. Bochner BH, Dalbagni G, Sjoberg DD, Silberstein J, Keren Paz GE, Donat SM, et al. Comparing Open Radical Cystectomy and Robot-assisted Laparoscopic Radical Cystectomy: A Randomized Clinical Trial. Eur Urol. 2015; 67: 1042-50. https://doi.org/10.1016/j.eururo.2014.11.043
7. Cheng CW, Wu TX, Shang HC, Li YP, Altman DG, Moher D, et al. CONSORT Extension for Chinese Herbal Medicine Formulas 2017: Recommendations, Explanation, and Elaboration. Ann Intern Med. 2017; 167: 112-21. https://doi.org/10.7326/M16-2977
8. Cortes JE, Khaled S, Martinelli G, Perl AE, Ganguly S, Russell N, et al. Quizartinib versus salvage chemotherapy in relapsed or refractory FLT3-ITD acute myeloid leukaemia (QuANTUM-R): a multicentre, randomised, controlled, open-label, phase 3 trial. The Lancet Oncology. 2019; 20: 984-97. https://doi.org/10.1016/s1470-2045(19)30150-0
9. Powles T, Durán I, van der Heijden MS, Loriot Y, Vogelzang NJ, De Giorgi U, et al. Atezolizumab versus chemotherapy in patients with platinum-treated locally advanced or metastatic urothelial carcinoma (IMvigor211): a multicentre, open-label, phase 3 randomised controlled trial. The Lancet. 2018; 391: 748-57. https://doi.org/10.1016/s0140-6736(17)33297-x
10. Sonpavde G, Shariat SF. Preoperative chemotherapy for bladder cancer: a standard waits to be optimally deployed. Cancer. 2012; 118: 8-11. https://doi.org/10.1002/cncr.26239
11. Zhang RJ, Wang ZJ, You WJ, Zhou FF, Guo ZC, Qian KY, et, al. Suppressive effects of plumbagin on the growth of human bladder cancer cells via pi3k/akt/mtor signaling pathways and emt. Cancer Cell International. 2020; 20(1), https://doi.org/10.1186/s12935-020-01607-y
12. Seca AML, Pinto D. Plant Secondary Metabolites as Anticancer Agents: Successes in Clinical Trials and Therapeutic Application. Int J Mol Sci. 2018; 19. https://doi.org/10.3390/ijms19010263
13. Qu Y, Chu B, Wei X, Lei M, Hu D, Zha R, et al. Redox/pH dual-stimuli responsive camptothecin prodrug nanogels for "on-demand" drug delivery. J Control Release. 2019; 296: 93-106. https://doi.org/10.1016/j.jconrel.2019.01.016
14. Qu Y, Safonova O, De Luca V. Completion of the canonical pathway for assembly of anticancer drugs vincristine/vinblastine in Catharanthus roseus. Plant J. 2019; 97: 257-66. https://doi.org/10.1111/tpj.14111

15. Qian K, Wang G, Cao R, Liu T, Qian G, Guan X, et al. Capsaicin Suppresses Cell Proliferation, Induces Cell Cycle Arrest and ROS Production in Bladder Cancer Cells through FOXO3a-Mediated Pathways. Molecules. 2016; 21. https://doi.org/10.3390/molecules21101406
16. Zhang R, Zhu X, Bai H, Ning K. Network Pharmacology Databases for Traditional Chinese Medicine: Review and Assessment. Front Pharmacol. 2019; 10: 123. https://doi.org/10.3389/fphar.2019.00123
17. Zhao Z, Yin JQ, Wu MS, Song G, Xie XB, Zou C, et al. Dihydromyricetin activates AMP-activated protein kinase and P38(MAPK) exerting antitumor potential in osteosarcoma. Cancer Prev Res (Phila). 2014; 7: 927-38. https://doi.org/10.1158/1940-6207.CAPR-14-0067
18. Fan KJ, Yang B, Liu Y, Tian XD, Wang B. Inhibition of human lung cancer proliferation through targeting stromal fibroblasts by dihydromyricetin. Mol Med Rep. 2017; 16: 9758-62. https://doi.org/10.3892/mmr.2017.7802
19. Wang F, Chen X, Yuan D, Yi Y, Luo Y. Golgi reassembly and stacking protein 65 downregulation is required for the anti-cancer effect of dihydromyricetin on human ovarian cancer cells. PLoS One. 2019; 14: e0225450. https://doi.org/10.1371/journal.pone.0225450
20. Wang Z, Sun X, Feng Y, Liu X, Zhou L, Sui H, et al. Dihydromyricetin reverses MRP2-mediated MDR and enhances anticancer activity induced by oxaliplatin in colorectal cancer cells. Anticancer Drugs. 2017; 28: 281-8. https://doi.org/10.1097/CAD.0000000000000459
21. Xu Y, Wang S, Chan HF, Lu H, Lin Z, He C, et al. Dihydromyricetin Induces Apoptosis and Reverses Drug Resistance in Ovarian Cancer Cells by p53-mediated Downregulation of Survivin. Sci Rep. 2017; 7: 46060. https://doi.org/10.1038/srep46060
22. Tieng FYF, Latifah SY, Md Hashim NF, Khaza'ai H, Ahmat N, Gopalsamy B, et al. Ampelopsin E Reduces the Invasiveness of the Triple Negative Breast Cancer Cell Line, MDA-MB-231. Molecules. 2019; 24. https://doi.org/10.3390/molecules24142619
23. Zhao Y, Liu H, Wang Z, Zhang Q, Li Y, Tian W, et al. Electrodeposition to construct mechanically robust chitosan-based multi-channel conduits. Colloids Surf B Biointerfaces. 2018; 163: 412-8. https://doi.org/10.1016/j.colsurfb.2018.01.002
24. Hu W, Wang Z, Zha Y, Gu X, You W, Xiao Y, et al. High Flexible and Broad Antibacterial Nanodressing Induces Complete Skin Repair with Angiogenic and Follicle Regeneration. Adv Healthc Mater. 2020: e2000035. https://doi.org/10.1002/adhm.202000035
25. Ge Q, Lu M, Ju L, Qian K, Wang G, Wu CL, et al. miR-4324-RACGAP1-STAT3-ESR1 feedback loop inhibits proliferation and metastasis of bladder cancer. Int J Cancer. 2019; 144: 3043-55. https://doi.org/10.1002/ijc.32036
26. Liu S, Yang Y, Qu Y, Guo X, Yang X, Cui X, et al. Structural characterization of a novel polysaccharide from Panax notoginseng residue and its immunomodulatory activity on bone marrow dendritic cells. Int J Biol Macromol. 2020; 161: 797-809. https://doi.org/10.1016/j.ijbiomac.2020.06.117
27. Wang Z, Hu W, Du Y, Xiao Y, Wang X, Zhang S, et al. Green Gas-Mediated Cross-Linking Generates Biomolecular Hydrogels with Enhanced Strength and Excellent Hemostasis for Wound Healing. ACS Appl Mater Interfaces. 2020; 12: 13622-33. https://doi.org/10.1021/acsami.9b21325

28. Zhao Y, Wang Z, Zhang Q, Chen F, Yue Z, Zhang T, et al. Accelerated skin wound healing by soy protein isolate-modified hydroxypropyl chitosan composite films. Int J Biol Macromol. 2018; 118: 1293-302. https://doi.org/10.1016/j.ijbiomac.2018.06.195
29. Zhou Q, Chen S, Lu M, Luo Y, Wang G, Xiao Y, et al. EFEMP2 suppresses epithelial-mesenchymal transition via Wnt/beta-catenin signaling pathway in human bladder cancer. Int J Biol Sci. 2019; 15: 2139-55. https://doi.org/10.7150/ijbs.35541
30. Zheng D-W, Dong X, Pan P, Chen K-W, Zhang X-Z. Phage-guided modulation of the gut microbiota of mouse models of colorectal cancer augments their responses to chemotherapy. Nature Biomedical Engineering. 2019; 3.
31. Laverty H, Meulien P. The Innovative Medicines Initiative -10 Years of Public-Private Collaboration. Front Med (Lausanne). 2019; 6: 275. https://doi.org/10.3389/fmed.2019.00275
32. Sharma SK, Shrivastava N, Rossi F, Tung LD, Thanh NTK. Nanoparticles-based magnetic and photo induced hyperthermia for cancer treatment. Nano Today. 2019; 29: 100795. https://doi.org/10.1016/j.nantod.2019.100795
33. Bojko A, Czarnecka-Herok J, Charzynska A, Dabrowski M, Sikora E. Diversity of the Senescence Phenotype of Cancer Cells Treated with Chemotherapeutic Agents. Cells. 2019; 8. https://doi.org/10.3390/cells8121501
34. Hu W, Wang Z, Xiao Y, Zhang S, Wang J. Advances in crosslinking strategies of biomedical hydrogels. Biomater Sci. 2019; 7: 843-55. https://doi.org/10.1039/c8bm01246f
35. Pietzak EJ, Zabor EC, Bagrodia A, Armenia J, Hu W, Zehir A, et al. Genomic Differences Between "Primary" and "Secondary" Muscle-invasive Bladder Cancer as a Basis for Disparate Outcomes to Cisplatin-based Neoadjuvant Chemotherapy. Eur Urol. 2019; 75: 231-9. https://doi.org/10.1016/j.eururo.2018.09.002
36. Liu B, Tan X, Liang J, Wu S, Liu J, Zhang Q, et al. ERRATUM: A reduction in reactive oxygen species contributes to dihydromyricetin-induced apoptosis in human hepatocellular carcinoma cells. Sci Rep. 2015; 5: 7940. https://doi.org/10.1038/srep07940
37. Tan M, Jiang B, Wang H, Ouyang W, Chen X, Wang T, et al. Dihydromyricetin induced lncRNA MALAT1-TFEB-dependent autophagic cell death in cutaneous squamous cell carcinoma. J Cancer. 2019; 10: 4245-55. https://doi.org/10.7150/jca.32807
38. Hu W, Wang Z, Xu Y, Wang X, Xiao Y, Zhang S, et al. Remodeling of inherent antimicrobial nanofiber dressings with melamine-modified fibroin into neoskin. J Mat Chem B. 2019; 7: 3412-23. https://doi.org/10.1039/c9tb00276f
39. Wu P, Xiao A, Zhao Y, Chen F, Ke M, Zhang Q, et al. An implantable and versatile piezoresistive sensor for the monitoring of human-machine interface interactions and the dynamical process of nerve repair. Nanoscale. 2019; 11: 21103-18. https://doi.org/10.1039/c9nr03925b
40. Liu WL, Liu T, Zou MZ, Yu WY, Li CX, He ZY, et al. Aggressive Man-Made Red Blood Cells for Hypoxia-Resistant Photodynamic Therapy. Adv Mater. 2018; 30: e1802006. https://doi.org/10.1002/adma.201802006

41. Liu WL, Zou MZ, Liu T, Zeng JY, Li X, Yu WY, et al. Cytomembrane nanovaccines show therapeutic effects by mimicking tumor cells and antigen presenting cells. Nat Commun. 2019; 10: 3199. https://doi.org/10.1038/s41467-019-11157-1
42. Kim H, Wang SY, Kwak G, Yang Y, Kwon IC, Kim SH. Exosome-Guided Phenotypic Switch of M1 to M2 Macrophages for Cutaneous Wound Healing. Adv Sci (Weinh). 2019; 6: 1900513. https://doi.org/10.1002/advs.201900513
43. Gao F, Tang Y, Liu WL, Zou MZ, Huang C, Liu CJ, et al. Intra/Extracellular Lactic Acid Exhaustion for Synergistic Metabolic Therapy and Immunotherapy of Tumors. Adv Mater. 2019; 31: e1904639. https://doi.org/10.1002/adma.201904639
44. Wang J, Dong Y, Li Y, Li W, Cheng K, Qian Y, et al. Designer Exosomes for Active Targeted Chemo-Photothermal Synergistic Tumor Therapy. Advanced Functional Materials. 2018; 28: 1707360. https://doi.org/10.1002/adfm.201707360
45. Chen L, Mou S, Li F, Zeng Y, Sun Y, Horch RE, et al. Self-Assembled Human Adipose-Derived Stem Cell-Derived Extracellular Vesicle-Functionalized Biotin-Doped Polypyrrole Titanium with Long-Term Stability and Potential Osteoinductive Ability. ACS Appl Mater Interfaces. 2019; 11: 46183-96. https://doi.org/10.1021/acsami.9b17015
46. Liang J, Wu J, Wang F, Zhang P, Zhang X. Semaphoring 4D is required for the induction of antioxidant stress and anti-inflammatory effects of dihydromyricetin in colon cancer. Int Immunopharmacol. 2019; 67: 220-30. http://doi.org/10.1016/j.intimp.201812025

Figures

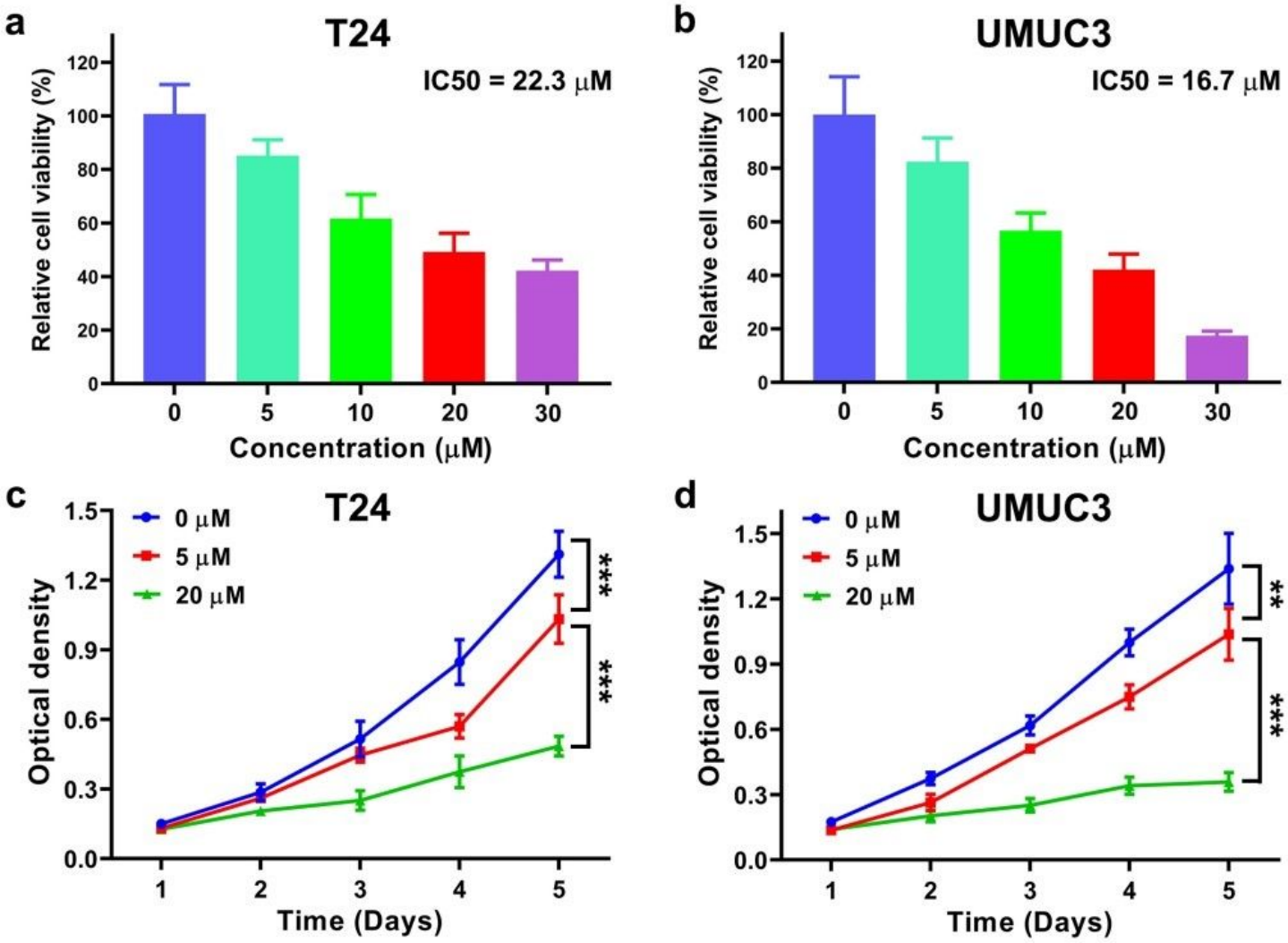

Figure 1

Dihydromyricetin (DHM) inhibited the viability and proliferation of MIBC (T24 and UMUC3) cells in vitro. (a, b) To determine the appropriate DHM concentration for in vitro tests, T24 and UMUC3 cells were co-incubated with DHM at a concentration of 0, 5, 10, 20 and 30 μM, respectively. The relatively cell viability were assessed by MTT assay, and the value of 50% inhibiting concentration (IC50) was calculated; (c, d) The MTT proliferation curves of T24 and UMUC3 cells which were incubated with DHM at 0, 5 and 20 μM for consecutive 5 days. **P < 0.01, ***P < 0.001.

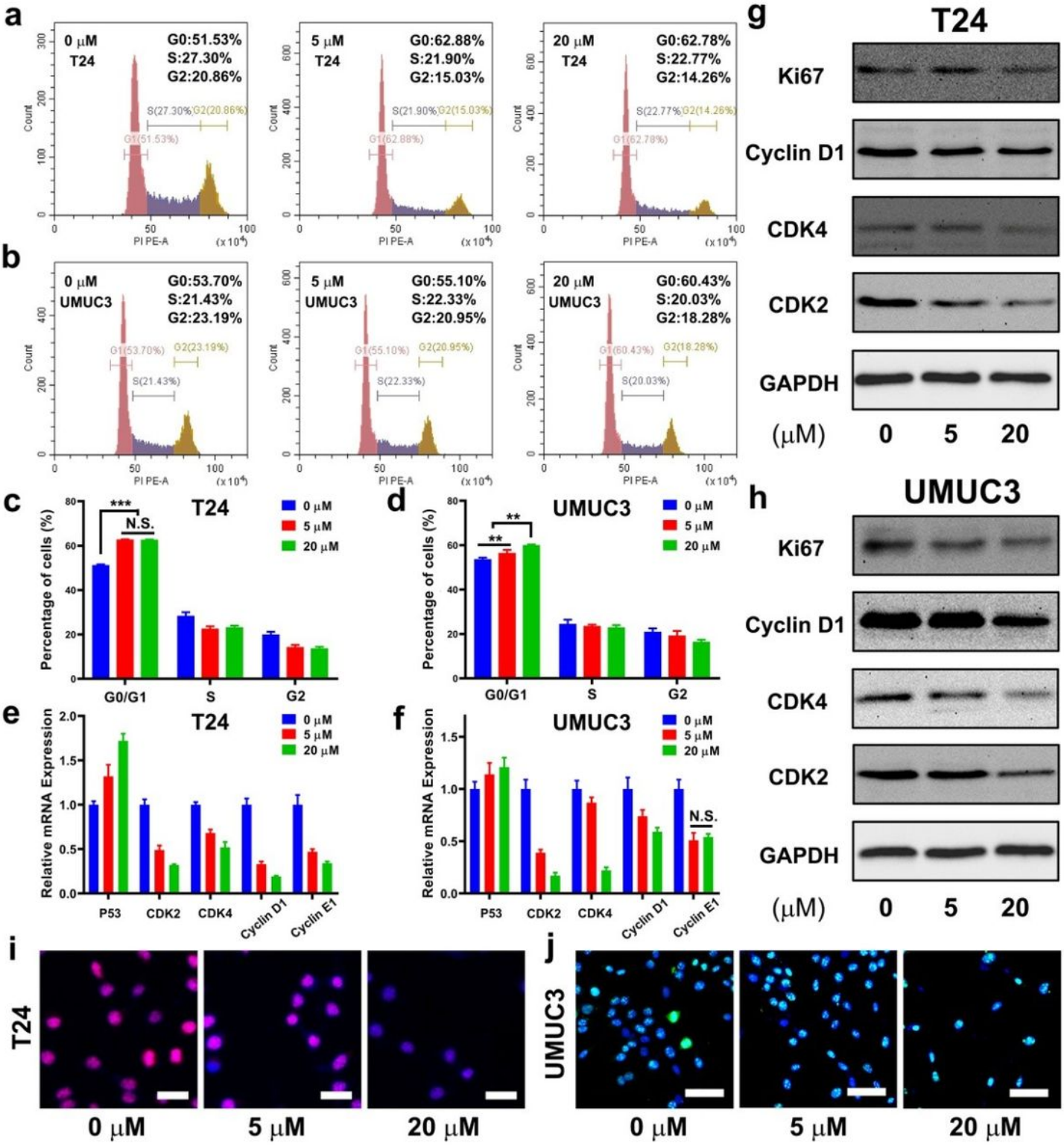

Figure 2

Dihydromyricetin (DHM) induced MIBC (T24 and UMUC3) cells cycle arrested in G0/G1 phase. (a, b) Representative flow cytometry images of cell cycle in MIBC cells after treated with DHM for 48 h; (c, d) Quantitative results of cell cycle distribution exhibited a significantly increase in G0/G1 phase cell percentages. **P < 0.01, ***P < 0.001; (e, f) The relative expression of cell cycle related genes (P53, CDK2, CDK4, Cyclin D1, Cyclin E1) in both kinds of cells could be modulated by DHM; (g. h) Western blot images

revealed an obvious down-regulation of cell cycle proteins, such as CDK2, CDK4, Cyclin D1 and Ki67; (i, j) Representative immunofluorescence (IF) images of Ki67 staining. Blue signal (DAPI): cell nucleus. Red/green signal: Ki67 protein. Scale bar: 100 μm.

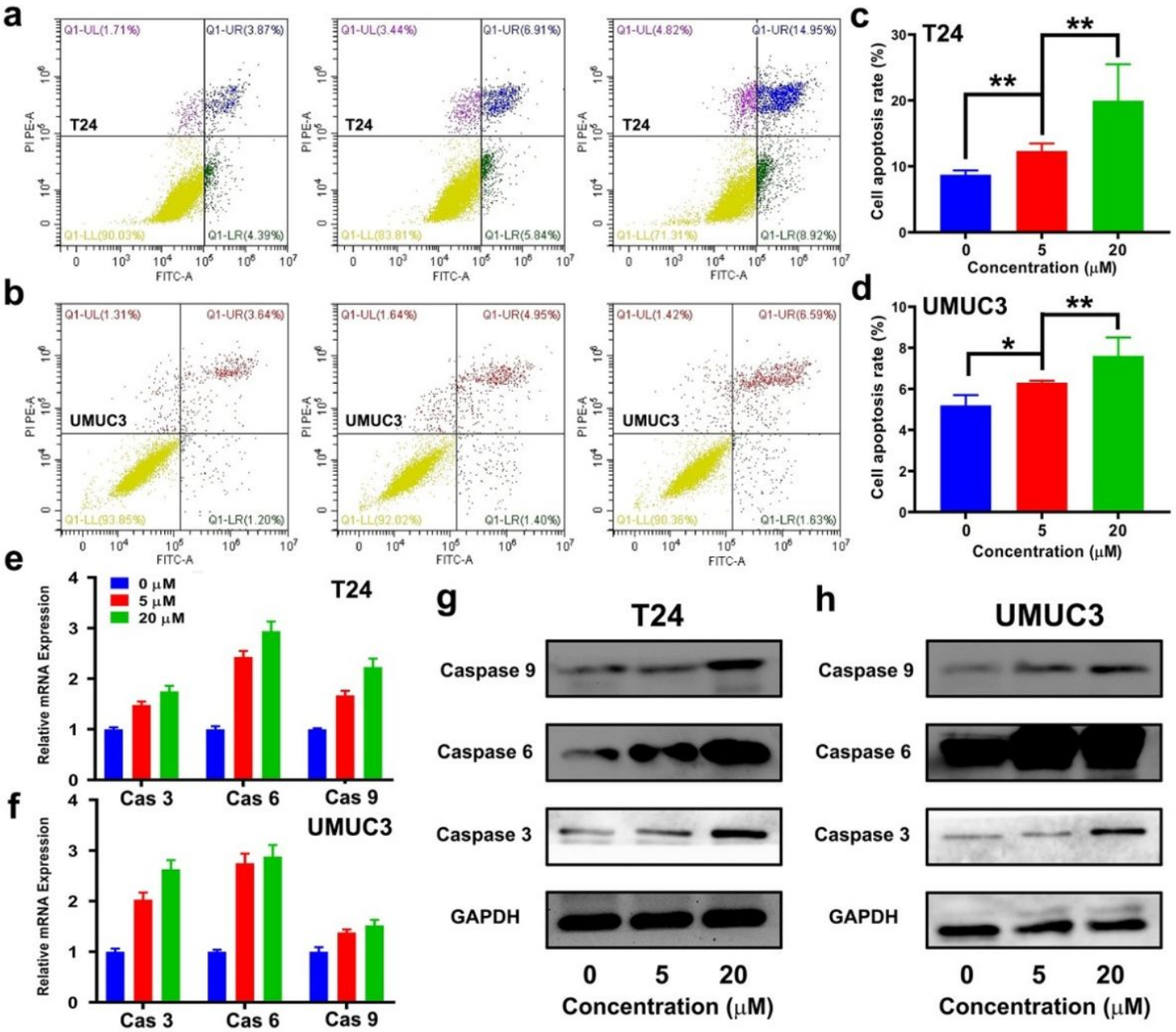

Figure 3

Dihydromyricetin (DHM) promoted MIBC (T24 and UMUC3) cells apoptosis. (a, b) Representative flow cytometry photos of apoptosis in T24 and UMUC3 cells after treated with DHM for 48 h; (c, d) Quantitative results of cell apoptosis rate exhibited an effectively pro-apoptotic activity of DHM. *P <0.05, **P < 0.01; (e, f) The relative expression of Caspase 3/6/9 in T24 and UMUC3 cells after DHM treatment; (g. h) Western blot images revealed a strong up-regulation of apoptosis proteins.

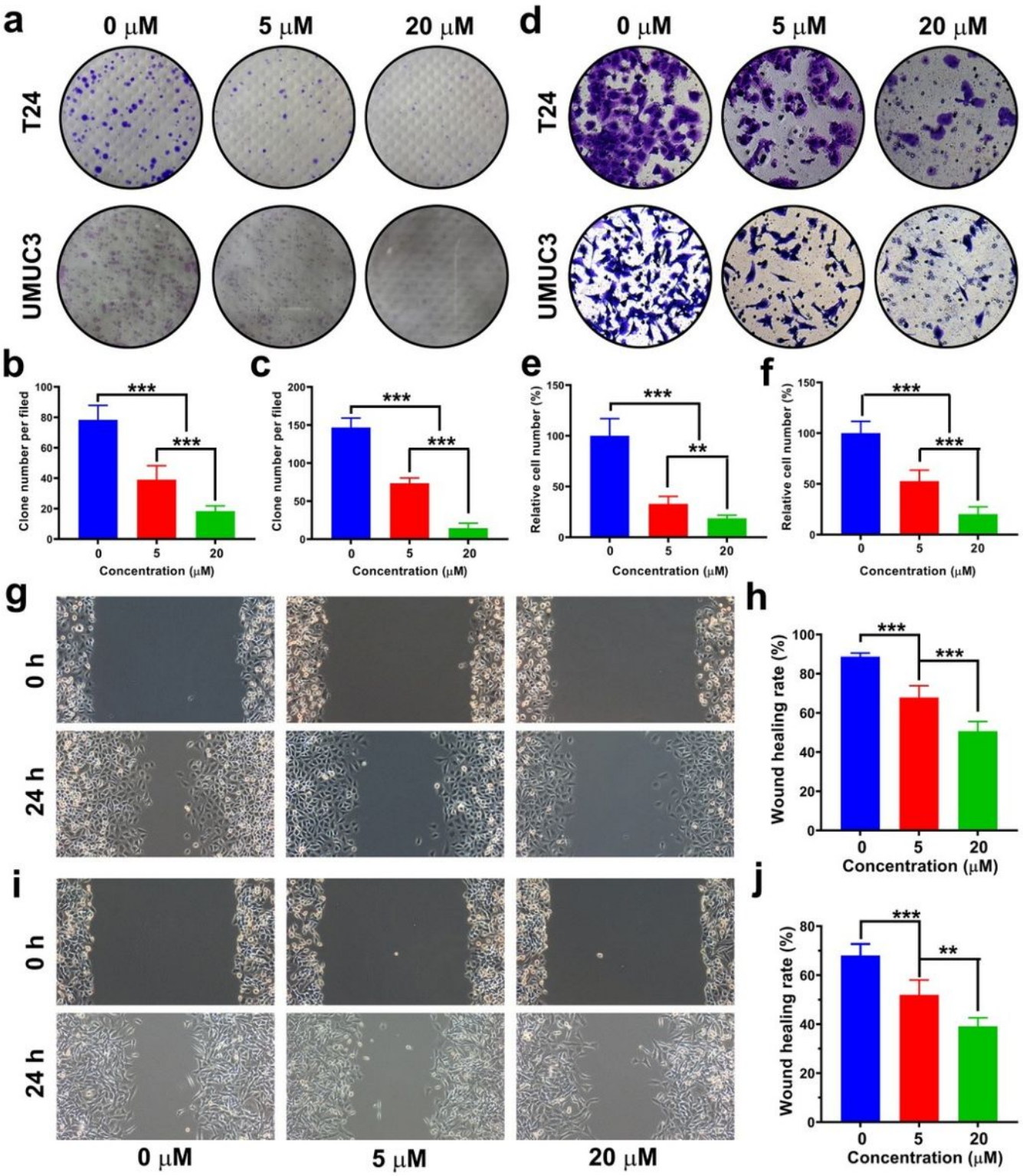

Figure 4

Dihydromyricetin (DHM) inhibited the migration and survival of MIBC (T24 and UMUC3) cells in vitro. (a) The influence of DHM on MIBC cell survival was evaluated by clonogenic survival assay; (b, c) Quantitative results of cell clone number per filed. ***P < 0.001; (d) Representative images of transwell chamber assay after DHM treatment. (e. f) Transwell chamber assay indicated that the migration ability of T24 and UMUC3 cells was significantly inhibited by DHM. **P < 0.01, ***P < 0.001; (g, h) The anti-

migration activity of DHM against T24 cell was investigated by wound healing assay; (i, j) The anti-migration activity of DHM against UMUC3 cell. **P < 0.01, ***P < 0.001.

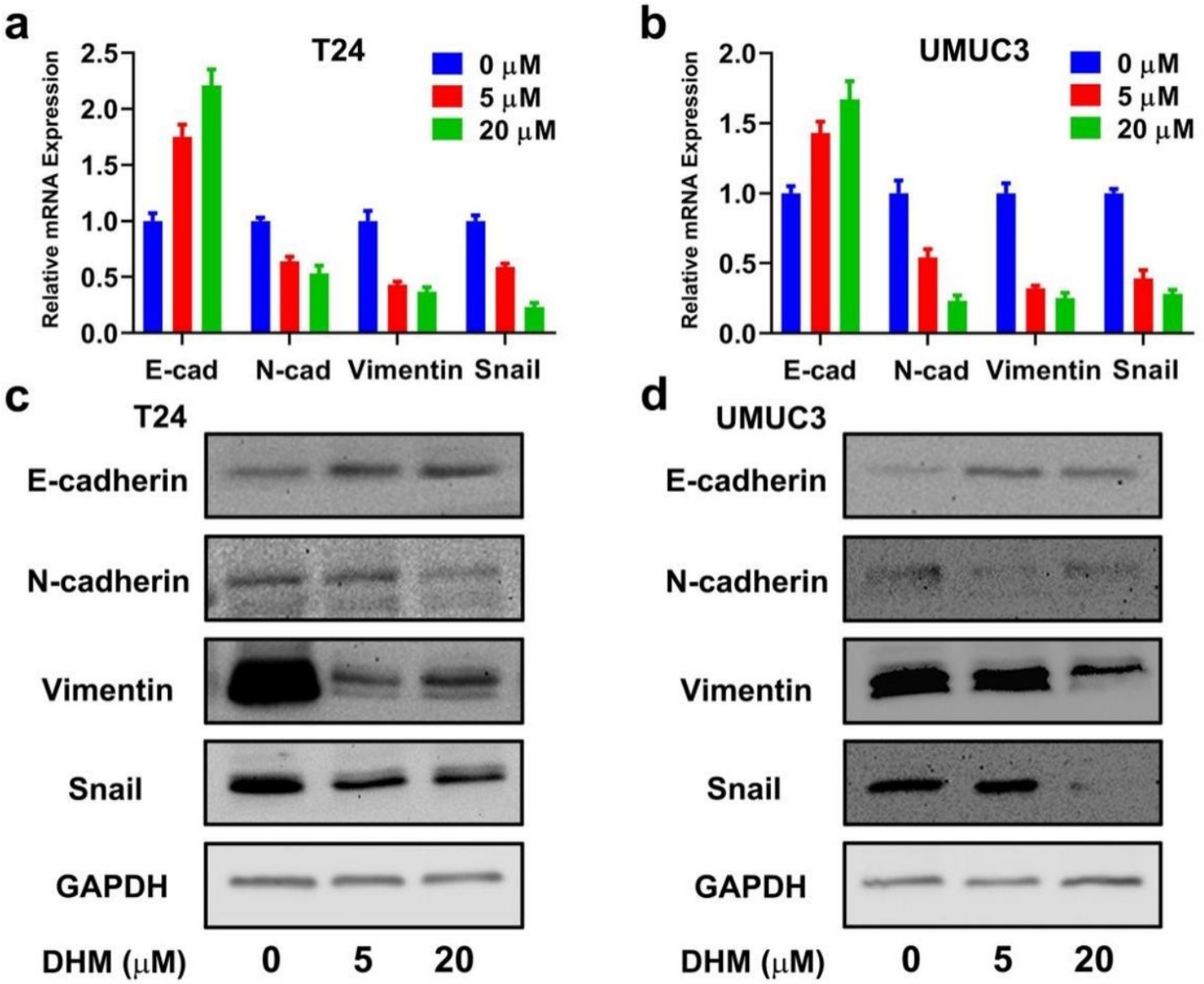

Figure 5

Epithelial-mesenchymal transition (EMT) pathway was blocked by DHM to inhibit MIBC cells migration. (a, b) The relative gene expression of EMT bio-markers (E-cad, N-cad, Vimentin, Snail) in T24 and UMUC3 cells, respectively; (c. d) E-cad protein expression was upregulated, N-cad, Vimentin and Snail protein expression was downregulated. These results indicated that DHM could block EMT pathway, and then cause the migration inhibition of MIBC cells directly.

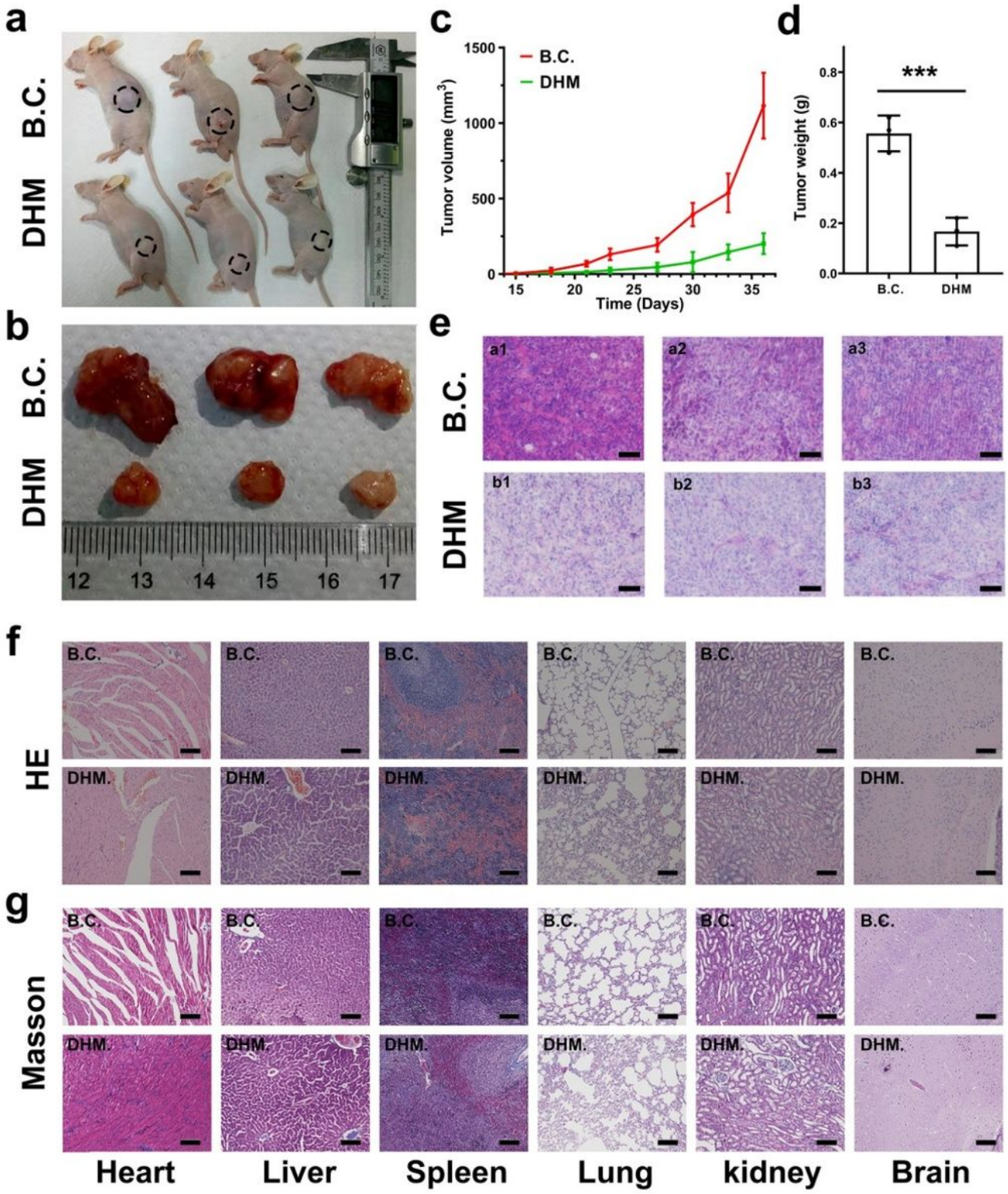

Figure 6

Dihydromyricetin (DHM) suppressed in vivo tumorigenesis with good biosafety. (a) BALB/c mice were seeded with T24 cell subcutaneously for 15 days. DHM and the control were then injected every third day for additional 21 days; (b) The photographs of tumor samples dissected from mice; (c) The growth curves of tumor volume from 15 th to 36 th day; (d) Quantitative results of tumor weight. ***P<0.001; (e) HE staining images of the tumor samples, a1-3 and b1-3 corresponding to the three individual animals in

the DHM group and control groups, respectively. Scale Bar: 100 μm; (f, g) Representative HE and Masson staining images of the organs (heart, liver, spleen, lung, kidney and brain) dissected from the treated mice. The results confirmed relatively good in vivo biosafety. Scale Bar: 100 μm.

Supplementary Files

This is a list of supplementary files associated with this preprint. Click to download.

- SI.docx